

Field performance of retaining walls reinforced with woven and nonwoven geotextiles

F. H. M. Portelinha¹, J. G. Zornberg² and V. Pimentel³

¹Associate Professor, Federal University of São Carlos, Civil Engineering Department - DECiv, Rodovia Washington Luis, km 235, mailbox 676, São Carlos, São Paulo, 13.565-905, Brazil, Telephone: +55 16 3351 82 62; Telefax: +55 16 3361 208; E-mail: fportelinha@ufscar.br

²Fluor Centennial Professor, The University of Texas at Austin, Civil Engineering Department – GEO, 1 University Station C1792 Austin, TX 78712-0280, USA, Telephone: +1 303 492 04 92; Telefax: +1 512 471 65 48; E-mail: zornberg@mail.utexas.edu

³Geotechnical Engineer, Geosolucoes Geotechnical and Environmental Engineering, Rua Simão Álvares, 912, Sao Paulo, SP, 05417-030, Brazil, Telephone: +55 11 3034 54 79; Telefax: +55 11 3812 66 83; E-mail: victor.pimentel@geosolucoes.com

Received 03 May 2013, revised 27 April 2014, accepted 22 May 2014

ABSTRACT: This paper presents an evaluation of the performance of two instrumented sections of a geosynthetic-reinforced soil wall, 5.6 m high, constructed using a lateritic fine-grained soil. Two sections with identical layout of a nonwoven and a woven geotextile were monitored for comparison purposes. The unconfined tensile stiffness of the nonwoven geotextile was three times smaller than that of the woven geotextile. This allowed direct evaluation of the effect of soil confinement on geotextile stiffness. Instrumentation was used to measure face displacements, reinforcement displacement and strains, and soil matric suction. Rainfall occurred both during and after construction, which facilitated evaluation of the effect of soil wetting on the walls performance. Ultimate and serviceability limit state analyses were conducted to gain further insight into the performance of the two walls. The results show that the performance of the section reinforced with nonwoven geotextile was equivalent to the one reinforced with woven geotextile, even after the observed reduction in matric suction after rainfall. For both sections, the overall deformations occurred during construction. Negligible deformations were observed during service. Maximum face displacements were measured in the lowest instrumented layer for the nonwoven geotextile section whereas it was in the highest layer for the woven geotextile section. These behaviours of face displacement distributions can be the result of the significant differences in global stiffness of the sections. Design analyses and field performance show that soil confinement has a beneficial effect on the nonwoven geotextile stiffness. The significant contribution of the soil cohesion of the lateritic soil played an important role in the behaviour of the nonwoven geotextile-reinforced wall.

KEYWORDS: Geosynthetics, Geotextile, Reinforced soil wall, Lateritic soils, Stiffness, Strains, Displacements

REFERENCE: Portelinha, F. H. M., Zornberg, J. G. and Pimentel, V. (2014). Field performance of retaining walls reinforced with woven and nonwoven geotextiles. *Geosynthetics International*, 21, No. 4, 270–284. [<http://dx.doi.org/10.1680/gein.14.00014>]

1. INTRODUCTION

Geosynthetic-reinforced soil (GRS) walls have been constructed using fine-grained local soils in countries such as Brazil, even though granular soils are recommended in guidelines of countries such as the United States (Elias and Christopher 1997; AASHTO 2002). The use of locally available soils has been reported to lead to significant cost savings in areas where granular materials are not available (Zornberg and Mitchell 1994; Stulgis 2005; Pathak and

Alfaro 2010). However, the use of fine-grained soils has also been reported to lead to the development of positive pore water pressures that have resulted in serviceability problems or failures (Koerner and Soong 2001; Stulgis 2005; Yoo and Jung 2006).

Soils available in tropical areas, many of which are classified as fine-grained, have shown good performance in geotechnical applications, often because of the presence of laterites, which show advantageous mechanical and

hydraulic properties (Futai *et al.* 2004; Osinubi and Nwaiwu 2005). In fact, the reported good performance of reinforced soil walls constructed using lateritic fine-grained soils has been surprisingly good, even after significant amounts of rainfall (Ehrlich *et al.* 1997; Benjamin *et al.* 2007; Portelinha *et al.* 2013). Recently, field and laboratory studies conducted by Riccio *et al.* (2014) reported that fine-grained tropical soils generate significant cohesion due to suction at field moisture and density, which has a significant effect on the tension in the reinforcement. This result may be considered typical of the tropical soil used in the construction of the wall. The backfill soil suction also has a significant influence on the soil-geotextile interface shear strength based on unsaturated pull-out tests (Esmaili *et al.* 2014).

For the case of fine-grained soils, a number of studies have shown that nonwoven geotextiles are a double function material (Fourie and Fabian 1987; Zornberg and Mitchell 1994; Tan *et al.* 2001; Noorzad and Mirmoradi 2010; Raisinghani and Viswanadham 2010, 2011). In these studies, in addition to the reinforcement function, nonwoven geotextiles provide internal drainage in the reinforced zone thus dissipating excessive pore water pressures and enhancing the internal stability of the structure. Other benefits are the improvement of tensile stiffness and creep behaviour of nonwoven geotextiles under soil confinement (McGown *et al.* 1982; Ling *et al.* 1992; Boyle *et al.* 1996; Mendes and Palmeira 2008; França and Bueno 2011; Santos *et al.* 2014).

Nine case studies of GRS walls with fine-grained soils reported by Miyata and Bathurst (2007) have shown good performance when good compaction and appropriate drainage are considered. In general, for conditions representative of good performance, these structures have shown reinforcement strains of not more than 3%. Design analyses of fine-grained soil structures using the AASHTO (2002) simplified method have been shown to lead to overestimated reinforcement loads. Accordingly, other methods such as the K-stiffness method (Bathurst *et al.* 2005, 2008) and variants have been developed to give more realistic load predictions for working stress conditions including walls constructed with fine-grained soils (Miyata and Bathurst 2007; Ahmadabadi and Ghanbari 2009; Ghanbari and Taheri 2012).

This paper reports the field monitoring results of a GRS wall constructed using lateritic fine-grained soils that includes sections reinforced with nonwoven and woven geotextiles. The project involves retaining structures constructed as part of a development in the *Bairro Novo* residential condominium in Campinas, Sao Paulo, Brazil. The structure is a 9 m-high reinforced soil wall with 1H: 10V batter, constructed using locally available lateritic fine-grained soils. The retaining structure was constructed along 300 m of a natural slope. A 4.5 m-high sloped embankment (1.5H: 1.0V) was constructed on top of the retaining wall to achieve the required design elevation. Figure 1 shows the GRS wall. The GRS wall was originally designed using woven geotextile reinforcement with a required tensile strength of 50 kN/m (Elias and Christopher 1997). Instruments were installed in a 5.6 m-

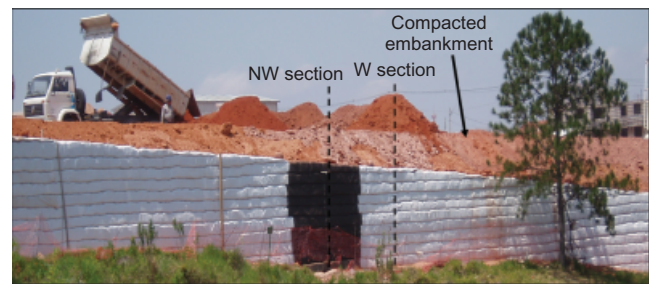


Figure 1. Photograph of the *Bairro Novo* GRS wall. NW, nonwoven; W, woven

high section of this wall for performance monitoring. However, for comparison purposes, a 5.6 m-high experimental section with nonwoven geotextiles and the same reinforcement layout was also fully instrumented. An interesting aspect of this study is that the nonwoven reinforcement had a tensile strength that was only 40% of that of the woven geotextile as well as an unconfined tensile stiffness (at 5% of strains) that was three times smaller. The purpose of this selection was to examine the effect of soil confinement on geotextile stiffness under operational conditions.

2. DESIGN CONSIDERATIONS

2.1. Soil properties and construction procedure

The use of locally available soils was motivated by the overall reduction of costs. The local soils used for the reinforced fill were obtained from a natural slope (Figure 2a). It consists of a dibasic lateritic non-plastic silty sand, with 33% fines (i.e. passing sieve no. 200). The particle size distribution of the soil is shown in Figure 3. Table 1 summarises the soil properties. The laboratory compaction characteristics of the soil were obtained from modified Proctor tests (ASTM D1557). The shear strength parameters were obtained using consolidated drained triaxial tests performed on saturated soil specimens (ASTM D7181). The foundation soil to a depth of 3 m was the same as the backfill soil.

Bags filled with manually compacted, locally available soil were used to construct the wrap-around facing (Figure 2b). Backfill specifications required a relative compaction of 95% and a placement moisture equal to the optimum water content ($\pm 2\%$) as obtained from modified Proctor tests. Compaction was achieved using a single drum vibratory roller (DYNAPAC Padfoot drum) for areas located at a distance beyond 1.0 m from the face (Figure 2c). Light compaction using hand-operated tampers was conducted in the vicinity of the face in order to minimise face displacements or local failures during construction (Figure 2d).

2.2. Geotextile selection and layout

A woven geotextile with an ultimate tensile strength of 57 kN/m was selected for the project. The experimental section involving nonwoven geotextile was selected to have a comparatively smaller strength of 25 kN/m. Wide-width tensile test results for both woven and nonwoven



Figure 2. Compaction process: (a) soil spreading; (b) soil bag facing; (c) compaction roller; (d) hand-operated tampers

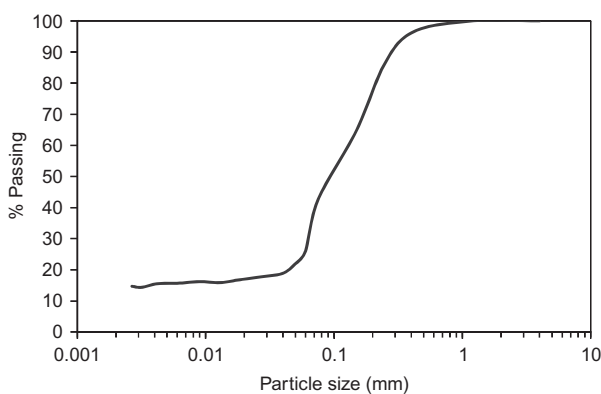


Figure 3. Particle size distribution of backfill soil material

geotextiles are given in Figure 4. Table 2 shows the physical and hydraulic properties of both reinforcement materials. The main motivation to select the mentioned nonwoven geotextile was to validate reported increases in the stiffness under confined conditions (e.g. McGown *et al.* 1982; Ling *et al.* 1992; Palmeira *et al.* 1996).

Table 1. Properties of the soil used as backfill material

Properties	Standard	Value
Specific gravity of solids	NBR 6508 (1984)	2.65
Liquid limit	NBR 6459 (1984)	32%
Plasticity index	NBR 7180 (1984)	Nonplastic
Maximum dry unit weight	ASTM D1557	19.4 kN/m ³
Optimum water content	ASTM D1557	11%
Cohesion	ASTM D7181	19 kPa
Friction angle	ASTM D7181	29°
Hydraulic conductivity	NBR 14545 (2000)	1.5 × 10 ⁻⁶ m/s

Furthermore, nonwoven geotextiles were expected to have hydraulic benefits when using fine-grained soils in relation to woven geotextiles under wetting conditions (Zornberg and Mitchell 1994).

Both instrumented sections were constructed with a reinforcement vertical spacing of 0.4 m and a reinforcement length of 7.0 m. A cross-section of the wall is illustrated in Figure 5. A wrap-around wall facing with sand

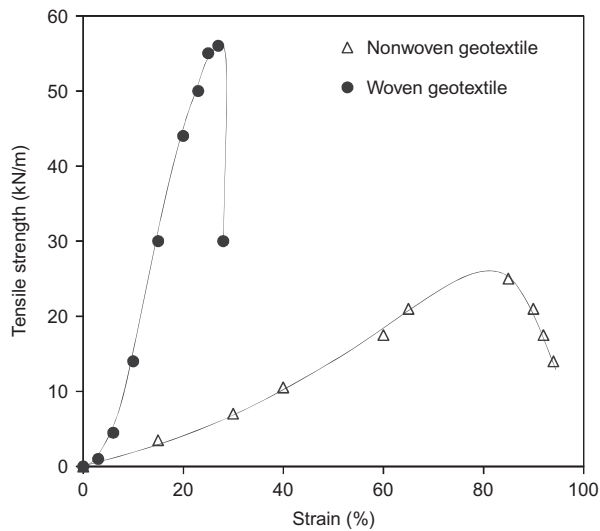


Figure 4. Wide-width tensile test results for the woven and nonwoven geotextiles (ASTM 4595)

bags was used. The soil bags also acted as the formwork during the construction process. To provide a natural appearance for the wall and the embankment, a vegetated face covering was adopted. Drainage channels were installed at the back of structure between the reinforced soil zone and the natural retained soil (Figure 5).

2.3. Comparison of design approaches

Ultimate limit state (ULS) and serviceability limit state (SLS) analyses were carried out to better understand the field monitoring results based on the predicted reinforcement tensile loads as well as the calculated factors of safety. The reduction factors adopted in the analyses to obtain the allowable tensile strength in the reinforcement layers are shown in Table 3, which was based on recommendations in BS8006 (2010). Internal stability regarding pull-out failure resulted in high factors of safety in comparison with those obtained for tensile rupture. External stability analyses against sliding, overturning, bearing capacity of the foundation and overall failure were also conducted. Factors of safety for these modes of failure were found to be adequate. Internal stability analyses with respect to reinforcement rupture were conducted according to Elias and Christopher (1997) using Coulomb active earth pressure approaches. Slope stability analyses were also conducted according to Spencer (1967). Slope stability analyses were conducted using the software program UTEXAS3 (Wright 1990) by the Uni-

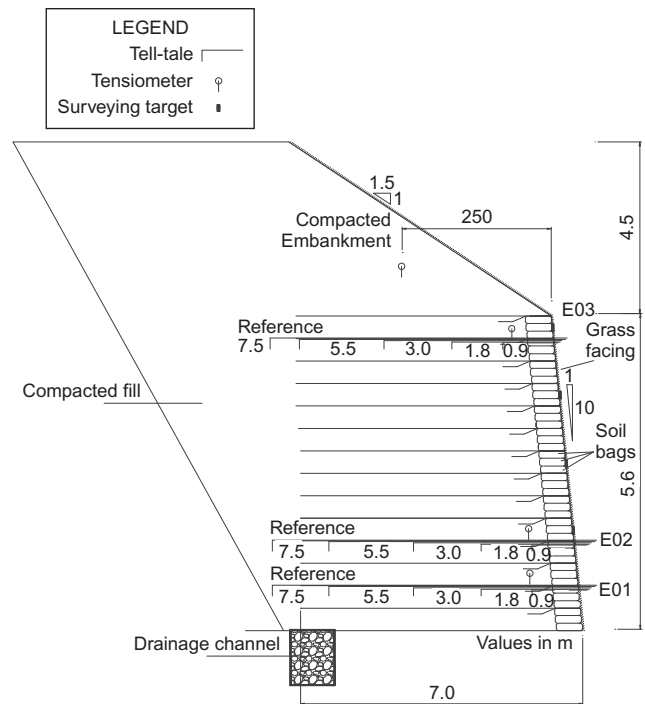


Figure 5. Cross-section of the experimental walls illustrating the instrumentation layout

Table 3. Reduction factors for ultimate limit state (ULS) and serviceability limit state (SLS) analyses (BS8006 (2010))

Reduction factor	Nonwoven geotextile	Woven geotextile
Installation damage	1.2	1.3
Creep*	1.2	1.1
Degradation	1.0	1.0

* Creep reduction factor of 1.0 was considered for SLS analyses.

versity of Texas at Austin, and the bilinear failure surface option. This software allows slopes and walls to be analysed with the reinforcement contribution and interpolation of positive and negative pore water pressures (matric suction) along the failure surface (Wright and Duncan 1991). Analyses were performed with and without soil cohesion, for the cases before and after the embankment construction. The assumptions and results of design analyses are summarised in Table 4. In general, analyses following Elias and Christopher (1997) and using the Coulomb method did not result in failure (exception for

Table 2. Properties of geotextile used in this study

Properties	Standard	Nonwoven geotextile	Woven geotextile
Weight per unit area	ASTM 5261	396 g/m ²	305 g/m ²
Polymer	-	Polyester filaments	Polypropylene yarns
Permittivity	ASTM 4491	1.05 s ⁻¹	0.04 s ⁻¹
Transmissivity	ASTM 4716	1.34 × 10 ⁻⁵ m ² /s	-
Apparent opening size	AFNOR G38-017 (1986)	75 µm	130 µm

Table 4. Ultimate limit state (ULS) analyses

Method	Assumptions	NW section		W section	
		FS _{breakage}	Failure surface	FS _{breakage}	Failure surface
Elias and Christopher (1997) using Coulomb failure surface	Zero cohesion, battered face, ULS	1.1	53°	2.6	53°
Elias and Christopher (1997) using Coulomb failure surface	30% of cohesion, battered face, ULS	1.4	53°	3.3	53°
Spencer slope stability ^a	Zero cohesion, battered face, ULS, bilinear surface	1.5	53° and 62° at 3.2 m from the base ^b	2.2	34° and 55° at 1.2 m from the base ^b
Spencer slope stability ^a	30% of cohesion, battered face, ULS, bilinear surface	1.8	48° and 56° at 2.8 m from the base ^b	2.4	24° and 45° at 1.6 m from the base ^b
Elias and Christopher (1997) using Coulomb failure surface	Zero cohesion, battered face, ULS	0.8	53°	1.8	51°
Elias and Christopher (1997) using Coulomb failure surface	30% of cohesion, battered face, ULS	1.0	53°	2.2	51°
Spencer slope stability ^a	Zero cohesion, battered face, ULS, bilinear surface	1.0	38° and 64° at 2.4 m from the base ^b	1.8	42° and 60° at 1.8 m from the base ^b
Spencer slope stability ^a	30% of cohesion, battered face, ULS, bilinear surface	1.2	41° and 73° at 1.8 m from the base ^b	2.0	40° and 56° at 1.2 m from the base ^b

^a Analyses conducted using UTEXAS3 (Wright 1990), with bilinear failure surfaces and overall failure.

^b Coordinates of the bilinear failure surface.

FS, factor of safety.

the conditions of zero cohesion and after embankment construction, FS = 0.8), although the factors of safety were close to 1.0. In the internal stability analyses of the woven geotextile section, the calculated factors of safety against rupture exceeded 1.0 for the various methods, even after embankment construction.

The SLS analyses were also conducted in this study. Serviceability limits for reinforced soil walls are typically established in terms of acceptable deformations. According to BS8006 (2010), SLS analyses suggests acceptable strains of 2%. In this study, 10% of face deformation was assumed as acceptable, since it corresponds to the value that the face batter becomes vertical. For SLS analyses, the allowable tensile strength for the calculation of the factor of safety corresponds to that related to the acceptable deformation (serviceability tensile strength) instead of ultimate tensile strength used for ULS analyses. The BS8006 (2010) recommends that serviceability tensile strength be obtained using isochronous load-strain curves from unconfined creep tests. However, in the case of nonwoven geotextiles, confined creep tests can better represent the actual condition of this type of reinforcement. Avesani (2013) conducted confined creep tests using the same nonwoven geotextile as that used in the current study, and measured an improvement of 90% in the reinforcement stiffness under confinement in sand. Isochronous load-strain curves from unconfined and confined creep tests of the nonwoven geotextile conducted by Avesani (2013) are presented in Figure 6. For woven geotextile reinforcement, SLS analyses were conducted using results from wide-width tensile tests. Table 5 summarises SLS analysis results. Results show that the service conditions assumed in SLS analyses are satisfied for woven section and for nonwoven section only if cohesion was maintained and without embankment construction. After construction of the embankment, larger

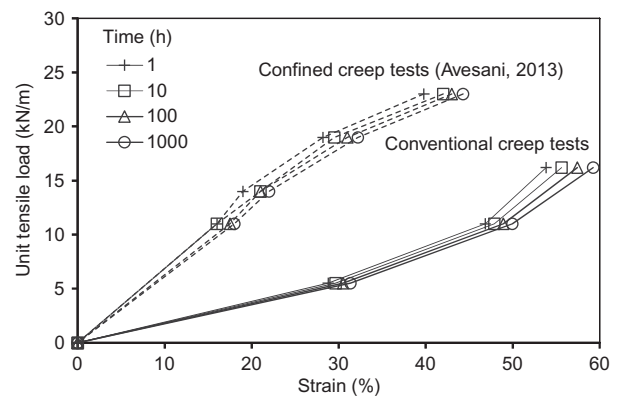


Figure 6. Isochronous load-strain curves from unconfined and confined nonwoven geotextile creep tests

displacements would be expected to occur in the NW wall.

3. WALL INSTRUMENTATION AND CONSTRUCTION

Instrumentation was used to monitor the wall during and after construction. Mechanical extensometers (tell-tales) with smooth-jacketed steel rods were installed along the reinforcement length, to monitor internal displacements. Face displacements were monitored using topographic surveys and matric suction was measured using mechanical tensiometers. The tensiometers used in this study had a plastic body that was 1.5 m long, a bourdon gage, ceramic cup with dimensions of 30 mm × 80 mm (diameter × height) and capacity of 90 kPa. Figure 5 shows the instrumentation layout used to evaluate the performance of the wall. The tell-tale points were attached to the geotextile at distances of 0.90, 1.80, 3.00 and 5.50 m from the

Table 5. SLS analyses

Method	Assumptions	Nonwoven geotextile section		Woven geotextile section	
		FS	Failure surface	FS	Failure surface
Before construction of the embankment					
BS8006 (2010) using Coulomb failure surface	100% of cohesion, battered face, SLS ($\epsilon = 10\%$), unconfined creep tests	0.4	53°	2.4 ^a	53°
BS8006 (2010) using Coulomb failure surface	100% of cohesion, battered face, SLS ($\epsilon = 10\%$), confined creep tests	1.0	53°	–	–
After construction of the embankment					
BS8006 (2010) using Coulomb failure surface	100% of cohesion, battered face, SLS ($\epsilon = 10\%$), unconfined creep tests	0.3	53°	1.9 ^a	53°
BS8006 (2010) using Coulomb failure surface	100% of cohesion, battered face, SLS ($\epsilon = 10\%$), confined creep tests	0.8	53°	–	–

^a Factors of safety (FS) calculated using wide-width tensile tests.

face and tensiometers were installed at 1.50 m from the face. One of the tell-tales was located outside the reinforced zone (natural fill), and relative measurements between these rods and rods located inside of the reinforced zone were taken. Relative displacements were measured using a digital caliper with a resolution of 0.01 mm. The accuracy and precision of the tell-tale system was previously tested in the field by comparing relative displacements of rods with positioning markers on the instrumented surfaces. This measurement system allowed measurements with accuracy of ± 3 mm and precision of ± 1 mm. Two instrumented wall sections are shown in Figure 7. Instruments were placed in three rows at different heights of 0.8, 1.6 and 5.0 m from the base of the wall (sets E01, E02 and E03, respectively), as illustrated in Figure 5. Survey targets were attached at the exposed wrap-around face at 1.6, 2.8, 4.0 and 5.2 m from the base of the wall for measurement of face displacements. Survey measurements had a resolution of 1 mm.

The construction of the entire structure from foundation preparation to final embankment construction took 86 days (from August 2010 to late January 2011). The reinforced wall construction started in September 2010

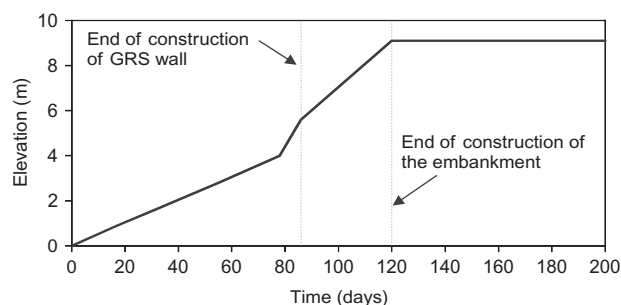
**Figure 7. View of two instrumented sections**

and finished in December 2010. After that, the embankment was constructed and the structure put in operation in late January 2011. Figure 8 shows the construction history.

4. PRECIPITATION AND ASSOCIATED SOIL WETTING

Precipitation data during and after construction (2010 to 2011) are presented in Figure 9. As shown in the figure, the reinforced wall was constructed in periods that received a number of periods of light rainfall. During the first month of construction (September 2010), 11 days of rainfall were registered, reaching a total precipitation of 110 mm. Up to the last months of construction of the reinforced structure, 13 days of rainfall occurred with an accumulated precipitation of 95 mm. The embankment was constructed during the heaviest rainfall period in that year, reaching an accumulated precipitation of 490 mm over 18 days.

The process of wetting of soil was monitored by tensiometers located at different heights and at 1.5 m from the face (Figure 5) and matric suction of the fill soil was monitored only in the nonwoven section. Tensiometer readings during and after construction are shown in Figure 10. A rapid reduction in matric suction occurred in the lowest reinforced layers and in the embankment after 40 days, which could be attributed to the previous contact with rainwater in these layers. Water infiltrated from the

**Figure 8. Construction history of the GRS wall and embankment**

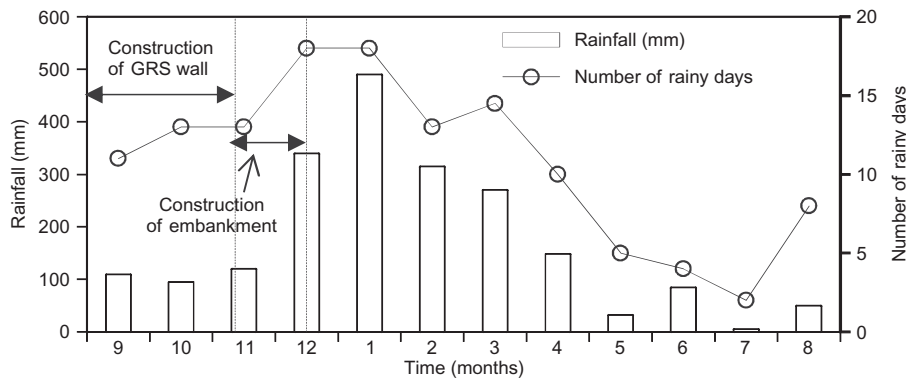


Figure 9. Precipitation data

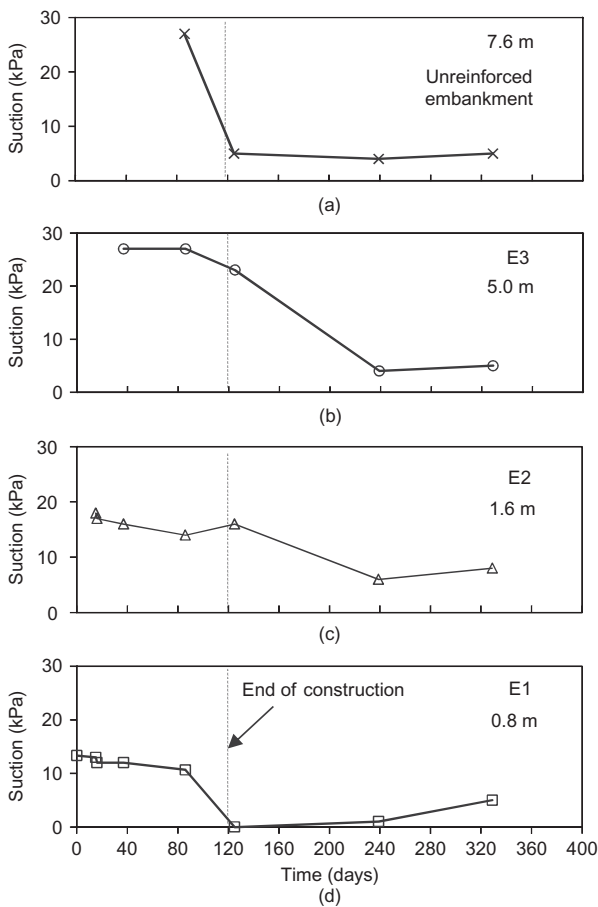


Figure 10. Tensiometer readings inside the geotextile-reinforced soil wall at elevation (a) 7.6 m, (b) 5.0 m, (c) 1.6 m and (d) 0.8 m

top of the wall to the base of the structure by passing over the exposed nonwoven geotextile wrap-around facing. For the other layers, water infiltrated through the reinforced soil by gravity. The infiltration started after 120 days, which corresponds to the period of heaviest precipitation of the year. In general, saturation of backfill was not reached, which could result in positive readings of pore water pressures. Minimum values of matric suction occurred in the instrumented row E01, with matric suction close to 0 kPa. For all layers, a minimum value of 5 kPa was measured after 240 days, which corresponds to work-

ing conditions of the wall (post-construction). Therefore, infiltration reached the wall toe after 240 days, with accumulated precipitation of 1700 mm and 107 rainy days. After this period, matric suction was observed to increase in all instrumented layers, which is indicative of drying, as drier periods were registered over this time.

5. DISPLACEMENTS OF THE REINFORCED SOIL WALLS

Results of horizontal displacement measurements along the reinforcement length of the nonwoven and woven sections are presented in Figures 11 and 12. Internal displacements are observed to increase in all instrumented rows, with higher rates during construction, especially at the monitored points located close to the face. After 120 days, which corresponds to the end of construction, no significant additional displacements were noticed. In general, displacements in the nonwoven section were higher than those in the W section.

Figure 13 presents a comparison between the maximum displacements recorded in the nonwoven and woven sections. Although displacements in the nonwoven section were higher than in the woven section, differences were small in the upper instrumented layers. However, in the lowest instrumented layer (row E01), the maximum displacement in the nonwoven section was twice that of the woven section. Yet, internal displacements were deemed comparatively small for practical purposes (normalised displacements of 0.01 m/m for the nonwoven section and 0.005 m/m for the woven section), mainly for the nonwoven geotextile structure. Post-construction displacements are negligible in both instrumented sections.

Figure 13b shows an increase and following decrease of displacement in the instrumented layer E02 (40th day), which suggests reinforcement tensile stress relief during construction. This behaviour may be attributed to the presence of equipment working in the vicinity of reinforcement layers close and above the instrumented layer E02. This statement is supported by the analytical method by Ghanbari and Taheri (2012) for calculating active earth pressure in reinforced retaining walls subject to a line surcharge. In this method, tensile forces tend to be more significant with proximity of the surcharge.

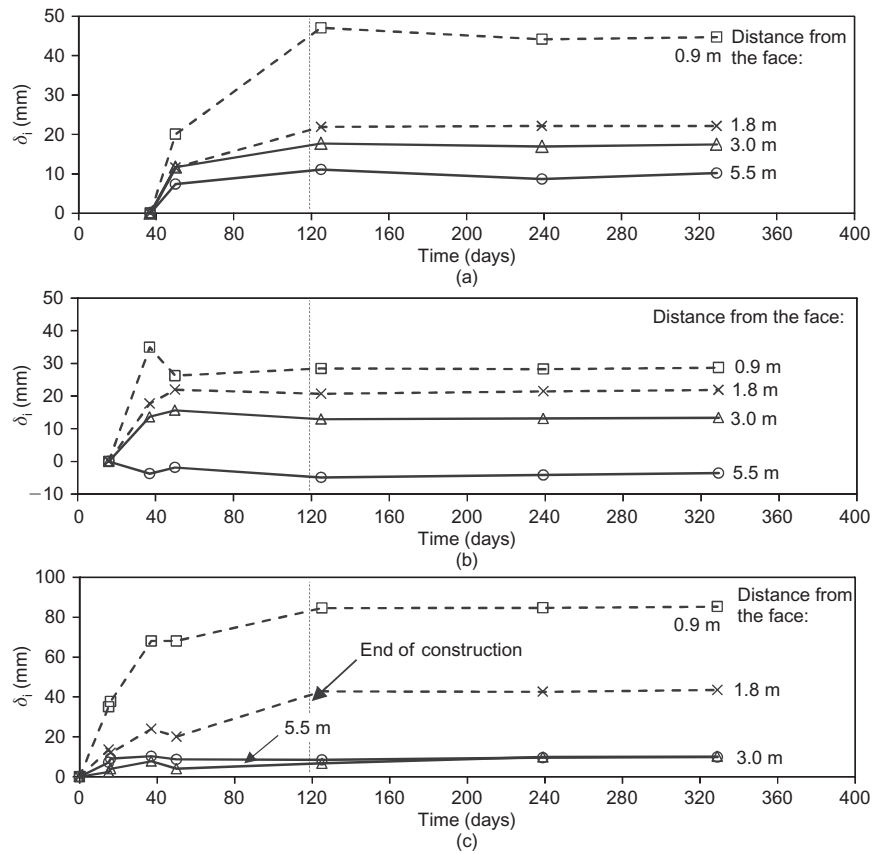


Figure 11. Internal displacements of nonwoven section at elevation (a) 5.0 m (E03), (b) 1.6 m (E02) and (c) 0.8 m (E01)

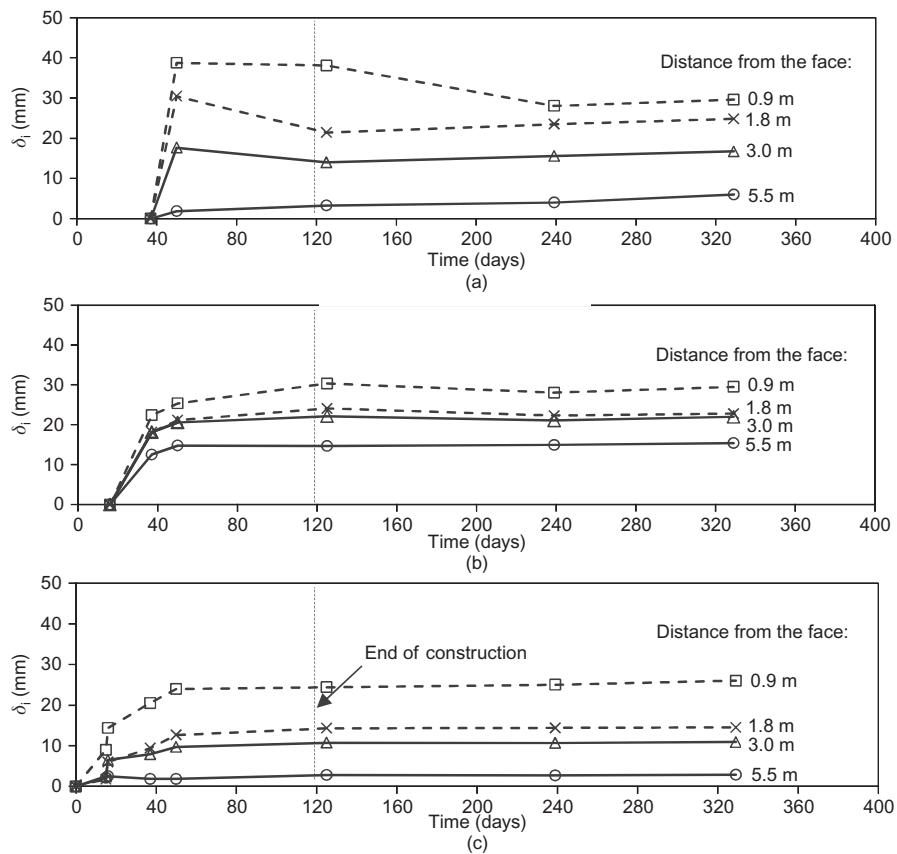


Figure 12. Internal displacements of woven section at elevation (a) 5.0 m (E03), (b) 1.60 m (E02) and (c) 0.8 m (E01)

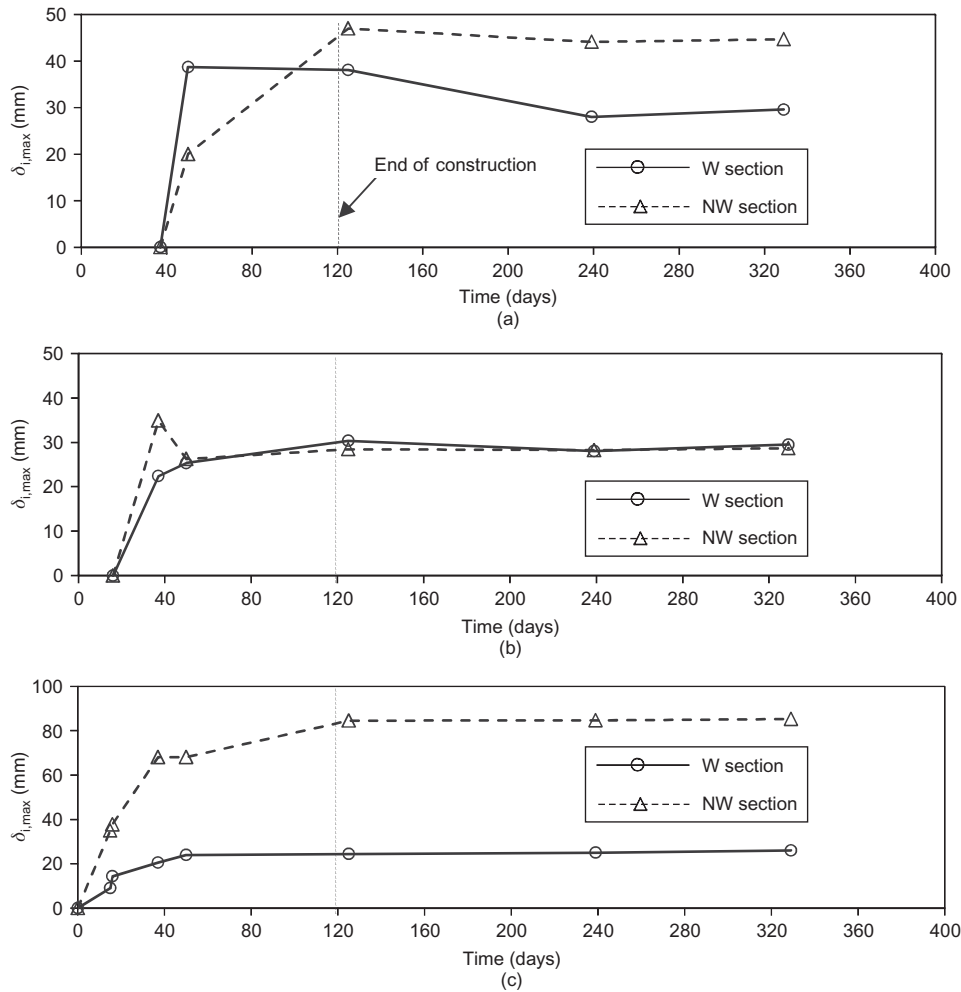


Figure 13. Maximum internal displacements of nonwoven (NW)- and woven (W)-reinforced sections at elevations: (a) 5.0 m (E03), (b) 1.6 m (E02) and (c) 0.8 m (E01)

Figure 14 presents the results of horizontal face displacement measurements. Higher face displacements occurred in the vicinity of the wall toe for the nonwoven section, whereas the highest displacements occurred in the

upper layers for the woven section. In fact, both SLS and ULS analyses resulted in the lowest factors of safety in the lower layers of the structures, which explains the behaviour of face displacements. In general, the maximum face displacements were higher for the nonwoven section, with values around 80 mm. The measured face displacements are consistent with results reported by Bathurst *et al.* (2010) and Berg *et al.* (2009) limits. As reported by Bathurst *et al.* (2010), the magnitude of face displacements are sensitive to the global stiffness of the wall; in this study the woven section has a much higher global stiffness than the nonwoven section.

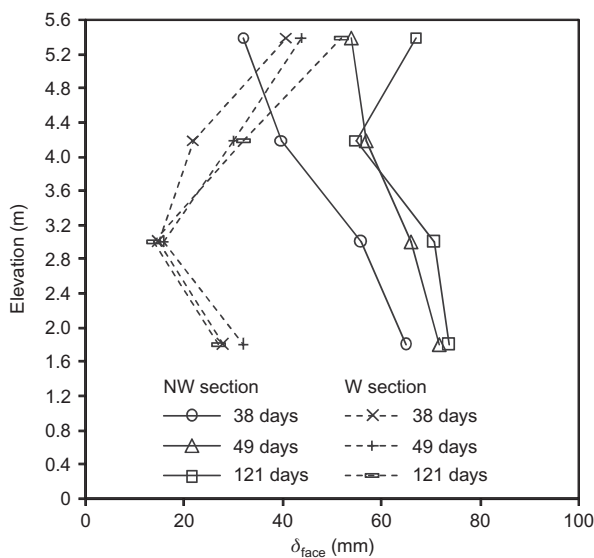


Figure 14. Face displacements for nonwoven (NW) and woven (W) sections

6. GEOTEXTILE STRAINS

The distribution of relative displacement along the reinforcement between the tell-tale points and the wall face is presented in Figure 15. In this figure, sigmoidal curves fitting the raw data are plotted in order to give a smooth representation of the distribution of displacements along the reinforcement length. A sigmoidal curve fit was used to evaluate the distribution of strains along the reinforcement by Zornberg and Arriaga (2003). The raw data for extensometer (tell-tale) displacement was initially smoothed by fitting the data to a sigmoidal curve, and the

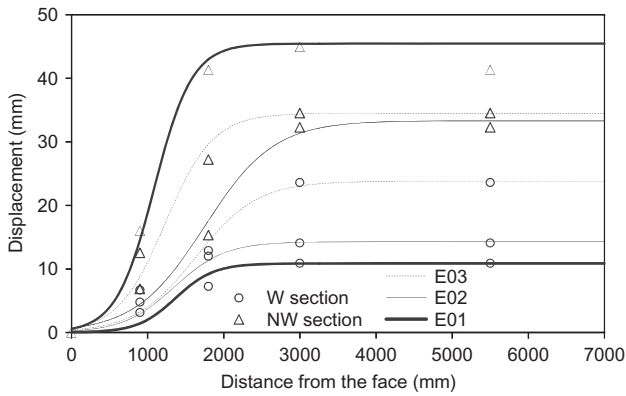


Figure 15. Distribution of relative displacements between tell-tale points and wall face along the geotextile length for nonwoven (NW) and woven (W) sections after 329 days

distribution of strains along the geotextile length was then computed by deriving the displacement function as

$$\epsilon = d \left(\frac{1}{a + be^{-cx}} \right) / dx \quad (1)$$

where d is the extensometer displacement, x is the distance from the face to the measured point, and a , b and c are parameters defined by the fitting of sigmoidal curves to the raw data using the least squares technique. Figures 16 and 17 show the distribution of strains for the nonwoven and woven sections. Both sections gave the same levels of strain under working conditions for instrumented rows E02 and E03. However, a significant discrepancy is observed in the lowest instrumented layer (E01), in which much larger strains were developed in the nonwoven section (up to 4.8%). This may be expected because horizontal stress increases toward the base of the wall and the stiffness of the nonwoven geotextile is considerably smaller than the woven geotextile.

Figure 18 shows a comparison of reinforcement strains between the nonwoven and woven sections. The major part of the strains was developed during construction. Maximum strain values of 4.8 and 3% were measured for nonwoven and woven sections, respectively. However, maximum strains were developed at 0.8 m from the base of the wall for the nonwoven section whereas these were

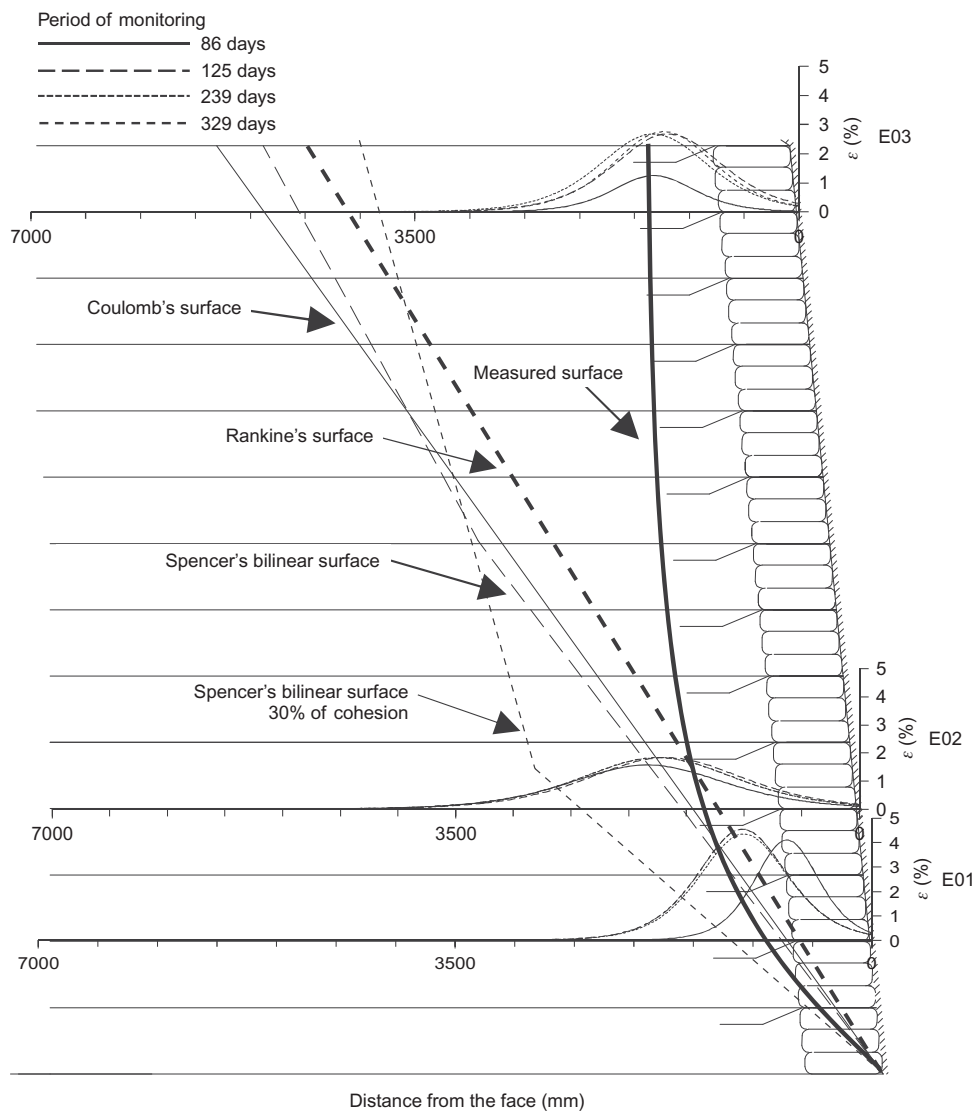


Figure 16. Geotextile strain distribution for nonwoven section in instrumented rows E01, E02 and E03

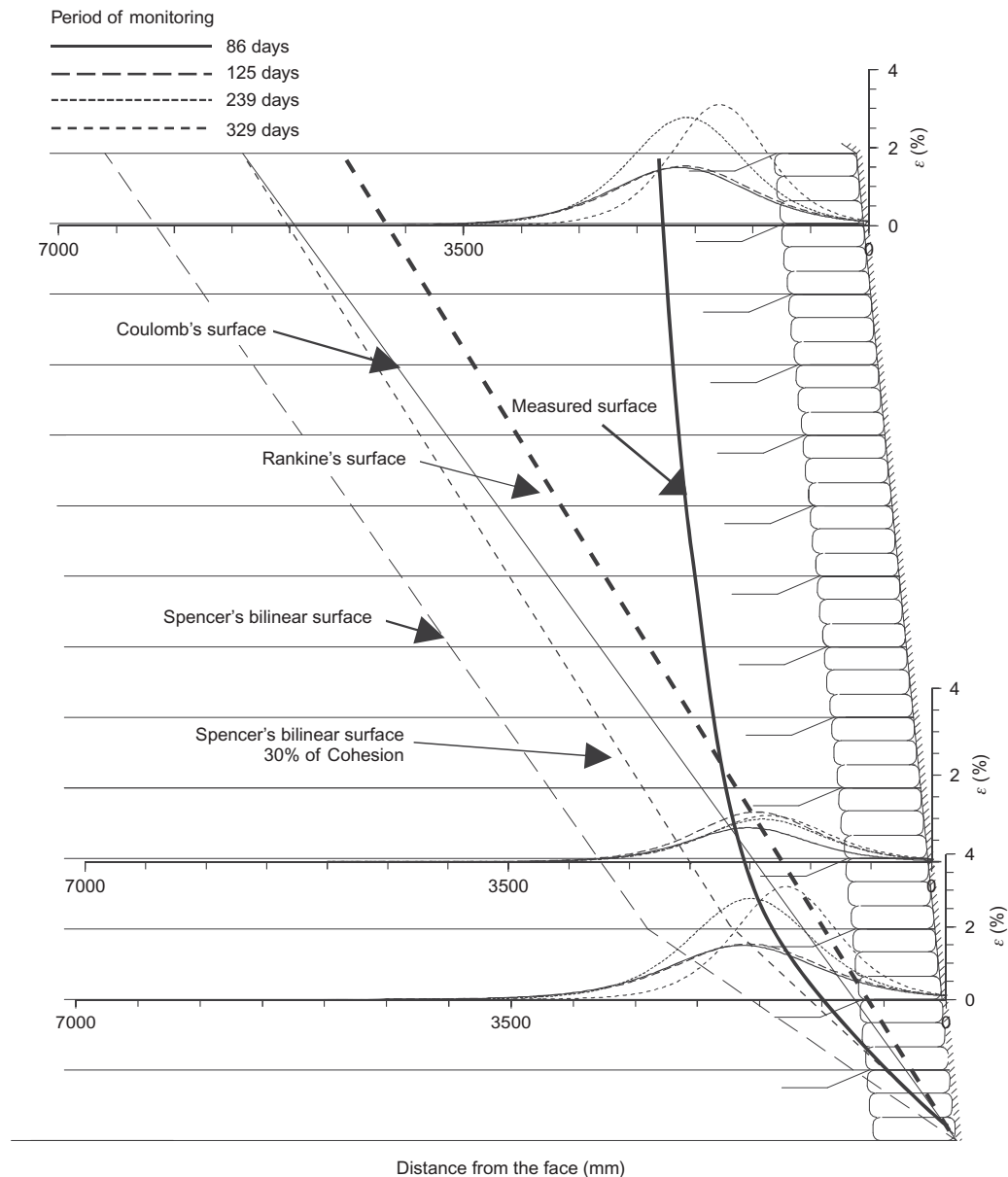


Figure 17. Geotextile strain distribution for woven section in instrumented rows E01, E02 and E03

observed at 5.0 m for the woven section. Higher strains in the nonwoven section were expected since the woven geotextile used in this structure was stiffer than the nonwoven geotextile. After construction, no additional displacements were registered in the nonwoven section. On the other hand, an additional strain of 0.5% of reinforcement was obtained in the woven section after a period of 239 days. Even though the matric suction increased after 240 days of operation, additional strains were observed for the woven geotextile (less permeable reinforcement) whereas no additional strains were developed for the nonwoven geotextile (more permeable reinforcement). This behaviour is attributed to the lower internal drainage capability of the reinforcement layers in the woven section than in the nonwoven section.

Figure 19 presents measured maximum peak strains for field walls in the current study and strains in geotextile retaining walls reported in the literature. Although the location of the maximum peak strain shows substantial

differences when compared to the other walls reported here, the structures reported by Tatsuoka and Yamauchi (1986) and Wu (1992) show similar peak locations and approximate levels of peak strains. In those cases in which the peak strain locations are not the same, the levels of strains are similar. For the woven geotextile section, the experimental structure reported by Won and Kim (2007) shows similar values of maximum peak strains. In many cases, nonwoven geotextiles and woven geotextiles-reinforced walls show similar levels of strains to those observed in the experimental sections presented in this work. This comparison is also useful to validate the instrumentation for internal displacement measurements used in this investigation, since the level of strains and location were consistent with other walls reported in the literature. The steel rods (tell-tales) used for internal displacement monitoring are inexpensive and a straightforward technique that can be used to easily monitor different reinforced soil walls.

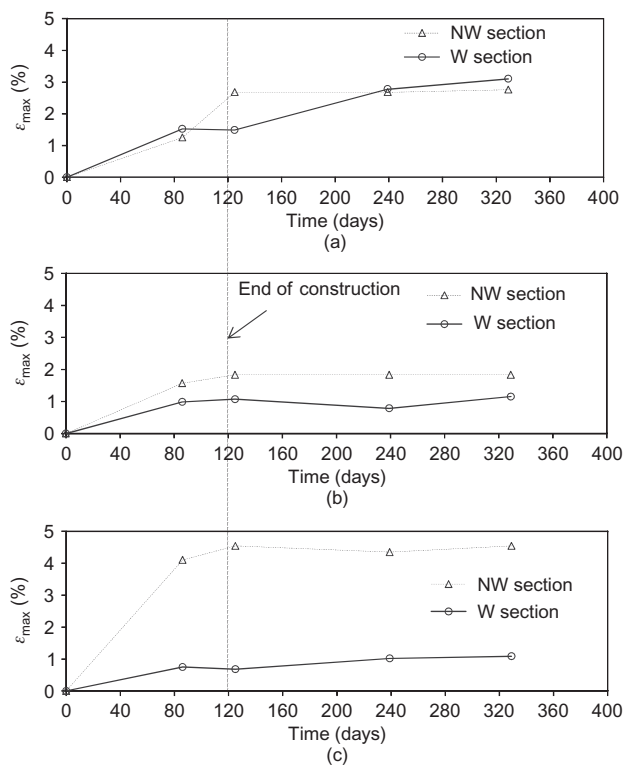


Figure 18. Evolution of peak reinforcement strains for nonwoven (NW)- and woven (W)-reinforced sections at elevation: (a) 5.0 m high (E03); (b) 1.6 m high (E02); (c) 0.80 m high (E01)

7. CONCLUSIONS

A performance comparison between woven and nonwoven GRS walls with fine-grained lateritic soil is reported in this paper. The effect of wetting and soil confinement are discussed herein. Based on the instrumentation results, the following conclusions can be drawn.

- The performance of the nonwoven section was similar to the woven section in terms of internal displacements and reinforcement strains, even though the nonwoven geotextile had an unconfined secant modulus (at 5% strain) three times lower than the woven geotextile. The field behaviour of the nonwoven geotextile section can be attributed to the effect of confinement of soil, resulting in smaller strains compared to the woven geotextile section. The lateritic cohesive soil used as the backfill for the walls in this study also played an important role in the overall field performance, due to the effective contribution of the soil cohesion due to matric suction.
- Readings of matric suction have shown the occurrence of wetting advancement into the nonwoven section during and after construction. However, changes in soil moisture and suction have not affected the overall wall performance, which is typical of lateritic fine-grained soils. Positive water pressures could not be registered in this study. After a certain period, the average suction of soil became

constant which was a positive contribution for the performance of both sections.

- Maximum displacements and reinforcement strains were located in the lowest instrumented layers for the nonwoven section, which is consistent with some measurements reported in the literature. For the woven geotextile (stiffer material), maximum displacements and reinforcement strains were located in the highest instrumented layer. Nonetheless, for the highest instrumented layer in the nonwoven geotextile section, maximum displacements and reinforcement strains were reported as still higher than in the woven section. As reported by Bathurst *et al.* (2010), global reinforcement stiffness has a significant influence on magnitude of facing displacements for reinforced soil walls.
- The failure surfaces obtained using maximum reinforcement strains were steeper than the calculated failure surfaces, particularly over the higher parts of the wall. This behaviour may be the result of construction stresses in the vicinity area of the steep wall face.
- Serviceability limit state analyses conducted in this study showed that using confined tensile properties of nonwoven geotextiles gave better estimates of field behaviour. However, the limit equilibrium approach was still conservative. Including soil cohesion in analyses also led to more realistic predictions of wall deformation.

Most of the displacement and deformation of the walls sections occurred during the construction period as reinforcement tensile load was mobilised due to compaction stresses and wall elevation. No significant deformations and displacements were noticed after construction even for the section with the nonwoven geotextile (lower stiffness). As a hypothesis, the significant contribution of soil cohesion of the lateritic soils was shown to play an important role in the performance of the wall. The beneficial effects of soil confinement of soil, and possibly the impregnation of particles in the nonwoven geotextile, were responsible for stiffness values similar to that of the woven geotextile. This hypothesis is supported by the similar behaviour of both wall sections.

NOTATION

Basic SI units given in parentheses.

a, b, c	sigmoid regression parameters (dimensionless)
H	height (m)
i	inclination (degree)
S	surcharge height (m)
x	relative displacement (m)
z	depth (m)
δ_{face}	face displacement (m)
δ_i	internal displacement (m)
$\delta_{i,\text{máx}}$	internal maximum displacement (m)
ε	reinforcement strains (dimensionless)
$\varepsilon_{\text{máx}}$	reinforcement peak strains (dimensionless)

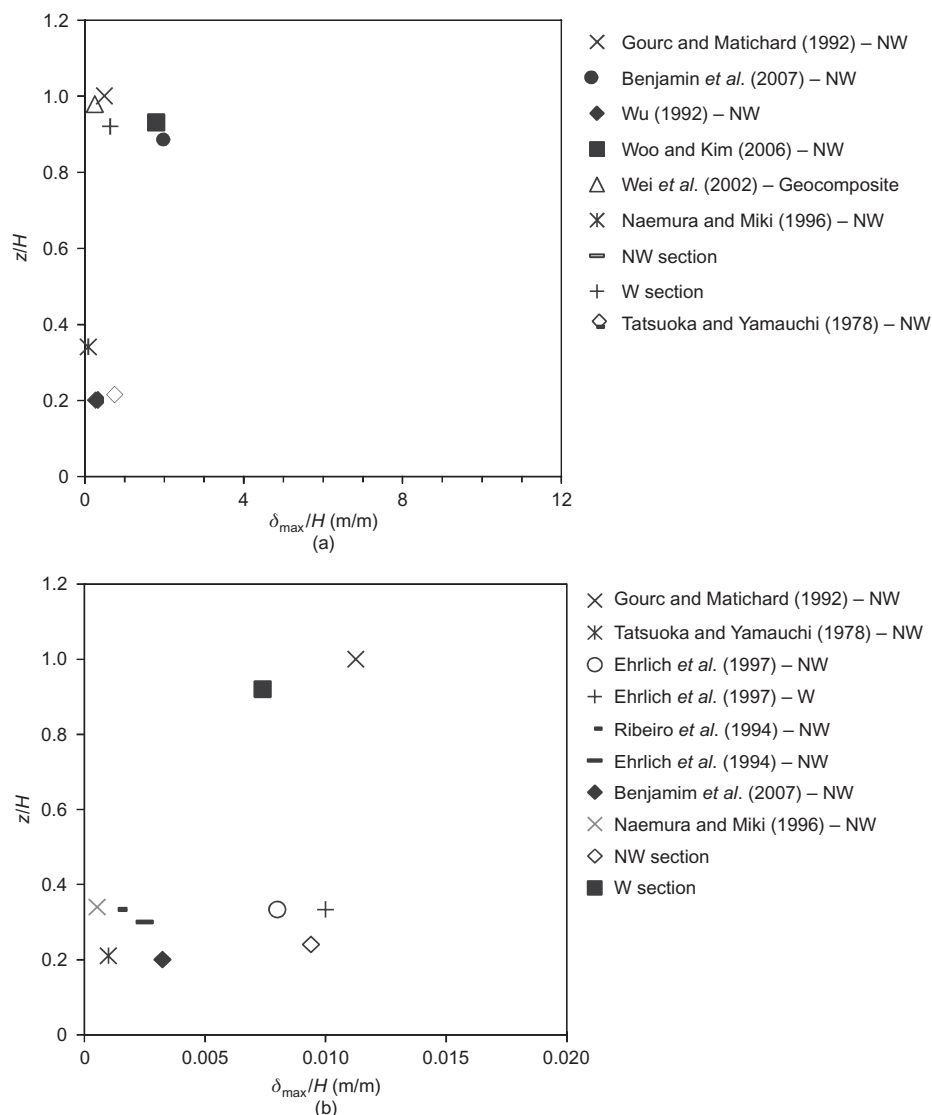


Figure 19. Comparison of displacements and reinforcement strains between cases reported in the literature: (a) normalised peak strains, (b) normalised displacements. NW, nonwoven; W, woven.

ABBREVIATIONS

- FS factor of safety
 SLS serviceability limit state
 ULS ultimate limit state

REFERENCES

- ASTM D1557. *Standard Test Methods for Laboratory Compaction Characteristic of Soil using Modified Effort*. ASTM International, West Conshohocken, PA, USA.
- ASTM D7181. *Method for Consolidated Drained Triaxial Tests for Soils*. ASTM International, West Conshohocken, PA, USA.
- ASTM 4595. *Standard Test Method for Tensile Properties of Geotextiles by Wide-width Strip Method*. ASTM International, West Conshohocken, PA, USA.
- ASTM 5261. *Standard Test Method for Measuring Mass per Unit Area of Geotextiles*. ASTM International, West Conshohocken, PA, USA.
- ASTM 4491. *Standard Test Methods for Water Permeability of Geotextiles by Permittivity*. ASTM International, West Conshohocken, PA, USA.
- ASTM 4716. *Standard Test Method for Determining the (in plane) Flow Rate per Unit Width and Hydraulic Transmissivity of a Geosynthetic using a Constant Head*. ASTM International, West Conshohocken, PA, USA.
- AFNOR G38–017 (1986). *FOS from Hydrodynamic Sieving*. AFNOR (Association Française de Normalisation) Committee on Geotextiles, La Plaine Saint-Denis, France.
- AASHTO (American Association of State Highway & Transportation Officials) (2002). *Standard Specifications for Highway Bridges*, 17th edition. AASHTO, Washington, DC, USA.
- Ahmadabadi, M. & Ghanbari, A. (2009). New procedure for active earth pressure calculation in retaining walls with reinforced cohesive-frictional backfill. *Geotextiles and Geomembranes*, **27**, No. 6, 456–463.
- Avesani, F. P. B. (2013). *Confined and Accelerated Creep Tests on Geosynthetics*. MSc thesis, Engineering School of Sao Carlos, University of São Paulo, Sao Paulo, Brazil, p. 134 (in Portuguese).
- Bathurst, R. J., Allen, T. M. & Walters, D. L. (2005). Reinforcement loads in geosynthetic walls and the case for a new working stress design method. *Geotextiles and Geomembranes*, **23**, No. 4, 287–322.
- Bathurst, R. J., Miyata, Y., Nernheim, A. & Allen, T. M. (2008). Refinement of K-stiffness method for geosynthetic reinforced soil walls. *Geosynthetics International*, **15**, No. 4, 269–295.
- Bathurst, R. J., Miyata, Y. & Allen, T. M. (2010). Invited keynote paper. Facing displacements in geosynthetic reinforced soil wall. *Earth*

- Retention Conference 3 (ER2010), Finno, R., Hashash, Y. M. A. & Arduino, P., Editors, ASCE, Reston, VA, USA, Geotechnical Special Publication no. 208, pp. 442–459.
- Benjamin, C. V. S., Bueno, B. & Zornberg, J. G. (2007). Field monitoring evaluation of geotextile-reinforced soil retaining walls. *Geosynthetics International*, **14**, No. 2, 100–118.
- Berg, R. R., Christopher, B. R. & Samtani, N. C. (2009). *Design of Mechanically Stabilized Earth Walls and Reinforced Soil Slopes – Volume I*. FHWA, Washington, DC, USA, FHWA-NHI-10-024.
- Boyle, S. M., Gallagher, M. & Holtz, R. D. (1996). Influence of strain rate, specimen length and confinement on measured geotextile properties. *Geosynthetics International*, **3**, No. 2 205–225.
- BS8006 (2010). *Code of Practice for Strengthened/reinforced Soils and other Fill*. British Standard Institution, London, UK, p. 260.
- Ehrlich, M., Vianna, A. J. D. & Fusaro, F. (1994). Performance of a reinforced soil wall. *Proceedings of the 10th Brazilian Conference on Soils Mechanics and Foundations*, Brazil, ABMS, Rio de Janeiro, Brazil, p. 819–824. (in Portuguese).
- Ehrlich, M., Vidal, D. & Carvalho, P. A. (1997). Performance of two geotextile reinforced soil slopes. *Proceedings of International Symposium on Recent Developments in Soil and Pavement Mechanics*, Rio de Janeiro, RJ, Brazil, Balkema, Rotterdam, the Netherlands, pp. 415–420.
- Elias, V. & Christopher, B. R. (1997). *Mechanically Stabilized Earth Walls and Reinforced Soil Slopes Design and Construction Guidelines*. FHWA, Washington, DC, USA, FHWA-SA-96-071.
- Esmaili, D., Hatami, K. & Miller, G. A. (2014). Influence of matric suction on geotextile reinforcement-marginal soil interface strength. *Geotextiles and Geomembranes*, **42**, No. 2, 139–153.
- Fourie, A. B. & Fabian, K. J. (1987). Laboratory determination of clay geotextile interaction. *Geotextiles and Geomembranes*, **6**, No. 4, 275–294.
- França, F. A. N. & Bueno, B. S. (2011). Creep behavior of geosynthetics using confined-accelerated tests. *Geosynthetics International*, **18**, No. 5, 242–254.
- Futai, M. M., Almeida, M. S. S. & Lacerda, W. A. (2004). Yield, strength and critical state conditions of a tropical saturated soil. *Journal of Geotechnical and Geoenvironmental Engineering*, **130**, No. 11, 1169–1179.
- Ghanbari, A. & Taheri, M. (2012). An analytical method for calculating active earth pressure in reinforced retaining walls subject to a line surcharge. *Geotextiles and Geomembranes*, **34**, No. 1, 1–10.
- Gourc, J. P. & Matichard, Y. (1992). Development of geotextile reinforcement technique in France – Application to retaining structures. *Proceedings of International Symposium on Geosynthetic reinforced soil retaining walls*, Netherland, pp. 131–152.
- Koerner, R. M. & Soong, T. Y. (2001). Geosynthetic reinforced segmental retaining walls. *Geotextiles and Geomembranes* **19**, No. 6, 359–386.
- Ling, H. I., Wu, J. T. H. & Tatsuoka, F. (1992). Short-term strength and deformation characteristics of geotextiles under typical operational conditions. *Geotextiles and Geomembranes*, **11**, No. 2, 185–219.
- McGown, A., Andrawes, K. Z. & Kabir, M. H. (1982). Load-extension testing of geotextiles confined in soil. *Proceedings of the 2nd International Conference on Geotextiles*, Las Vegas, NV, USA, IFAI, Roseville, MN, USA, vol. 2, pp. 793–798.
- Mendes, M. J. A. & Palmeira, E. M. (2008). Effects of confinement and impregnation on nonwoven geotextiles mechanical behavior. *Proceedings of the 1st Panamerican Geosynthetics Conference and Exhibition*, Cancun, Mexico, Transportation Research Board, Washington, DC, USA, pp. 540–545.
- Miyata, Y. & Bathurst, R. J. (2007). Development of K-stiffness method for geosynthetic reinforced soil walls constructed with $c-\phi$ soils. *Canadian Geotechnical Journal*, **44**, No. 12, 1391–1416.
- Naemura, S. & Miki, H. (1996). Design and construction of geotextiles reinforced soil structures for road earthworks in Japan. *Geosynthetics International*, **3**, No. 1, 49–62.
- NBR 6459 (1984). *Solo – Determinação do Limite de Liquidez*. Associação Brasileira de Normas Técnicas, Rio de Janeiro, Brazil (in Portuguese).
- NBR 6508 (1984). *Grãos de Solos que Passam na Peneira de 4,8 mm – Determinação da Massa Específica*. Associação Brasileira de Normas Técnicas, Rio de Janeiro, Brazil (in Portuguese).
- NBR 7180 (1984). *Solo – Determinação do Limite de Plasticidade*. Associação Brasileira de Normas Técnicas, Rio de Janeiro, Brazil (in Portuguese).
- NBR 14545 (2000). *Solo – Determinação coeficiente de permeabilidade de solos argilosos a carga variável*. Associação Brasileira de Normas Técnicas, Rio de Janeiro, Brazil (in Portuguese).
- Noorzad, R. & Mirmoradi, S. H. (2010). Laboratory evaluation of the behavior of geotextile-reinforced clay. *Geotextile and Geomembranes*, **28**, No. 4, 386–392.
- Osinubi, K. & Nwaiwu, C. (2005). Hydraulic conductivity of compacted lateritic soil. *Journal of Geotechnical and Geoenvironmental Engineering*, **131**, No. 8, 1034–1041.
- Palmeira, E. M., Tupa, N. & Gomes, R. C. (1996). In-soil tensile behaviour of geotextiles confined by fine soils. *Proceedings of the International Symposium on Earth Reinforcement, IS Kyushu-96*, Fukuoka, Japan, Ochiai, H., Yasufuku, N. & Omine, K., Editors, Balkema, Rotterdam, the Netherlands, vol. 1, pp. 129–132.
- Pathak, Y. P. & Alfaro, M. C. (2010). Wetting-drying behavior of geogrid-reinforced clay under working load conditions. *Geosynthetics International*, **17**, No. 3, 144–156.
- Portelinha, F. H. M., Bueno, B. S. & Zornberg, J. G. (2013). Performance of nonwoven geotextile reinforced soil walls under wetting conditions: laboratory and field investigation. *Geosynthetics International* **20**, No. 2, 90–104.
- Raisinghani, D. V. & Viswanadham, B. V. S. (2010). Evaluation of permeability characteristics of a geosynthetic-reinforced soil through laboratory tests. *Geotextiles and Geomembranes*, **28**, No. 6, 579–588.
- Raisinghani, D. V. & Viswanadham, B. V. S. (2011). Centrifuge model study on low permeable slope reinforced by hybrid geosynthetics. *Geotextiles and Geomembranes*, **28**, No. 6, 579–588.
- Ribeiro, T. S. M. T., Vicenzo Jr, M. C. & Pires, J. V. (1999). Behavior of a geosynthetic reinforced embankment in Belverede, Brazil. *Brazilian Conference on Geology*, Sao Pedro, AGBE, Sao Paulo, Brazil, vol. 9 (in Portuguese).
- Riccio, M., Ehrlich, M. & Dias, D. (2014). Field monitoring and analyses of the response of a block-faced geogrid wall using fine-grained tropical soils. *Geotextiles and Geomembranes*, **42**, No. 2, 127–138.
- Santos, E. G., Palmeira, E. M. & Bathurst, R. J. (2014). Performance of two geosynthetic reinforced walls with recycled construction waste backfill and constructed on collapsible ground. *Geosynthetics International*, **21**, No. 4, 256–269.
- Spencer, E. (1967). A method of analysis of stability o embankments assuming parallel inter-slice forces. *Geotechnique*, **17**, No. 1, 11–26.
- Stulgis, R. P. (2005). Full-scale MSE test walls. *Proceedings of the NAGS 2005/GRI-19 Conference*, Las Vegas, NV, USA, Geosynthetic Education Institute, Folsom, PA, USA, CD-ROM.
- Tan, S. A., Chew, S. H., Ng, C. C., Loh, S. L., Karunaratne, G. P. & Delmas Ph Loke, K. H. (2001). Large-scale drainage behavior of composite geotextile and geogrid in residual soil. *Geotextiles and Geomembranes* **19**, No. 3, 163–176.
- Tatsuoka, F. & Yamauchi, H. (1986). A reinforcing method for steep clay slopes using a non-woven geotextile. *Geotextile and Geomembranes*, **4**, No. 4, 241–268.
- Wei, J., Chua, K. C., Lim, S. K., Chew, S. H., Karunaratne, G. P., Tan, S. A. & Seah, Y. T. (2002). Performance of a geosynthetics reinforced steep slope in residual soil. *Proceedings of the 7th ICG*, Nice, France, Swets & Zeitlinger, Lisse, the Netherlands, pp. 325–328.
- Won, M. & Kim, Y. (2007). Internal deformation behavior of geosynthetic-reinforced soil walls. *Geotextiles and Geomembranes*, **25**, No. 1, 10–22.
- Wright, S. G. (1990). UTEXAS3. *A Computer Program for Slope Stability Analyses Calculation*, Shinoak Software, Austin, TX, USA.
- Wright, S. G. & Duncan, J. M. (1991). Limit equilibrium stability analyses for reinforced slopes. *Transportation Research Record*, **1330**, 40–46.
- Wu, X. X. (1992). Measured behavior of the Denver Walls. In *Geosynthetic-reinforced Soil Retaining Walls*, J. T. H. Wu, Editor, Balkema, Rotterdam, the Netherlands, pp. 31–42.

- Yoo, C. & Jung, H. Y. (2006). Case history of geosynthetic reinforced segmental retaining wall failure. *Journal of Geotechnical and Geoenvironmental Engineering, ASCE*, **132**, No. 12, 1538–1548.
- Zornberg, J. G. & Arriaga, F. (2003). Strain distribution within geosynthetic-reinforced slopes. *Journal of Geotechnical and Geoenvironmental Engineering*, **129**, No. 1, 32–34.
- Zornberg, J. G. & Mitchell, J. K. (1994). Reinforced soil structures with poorly draining backfills, Part I: reinforcement interactions and functions. *Geosynthetics International*, **1**, No. 2, 103–148.

The Editor welcomes discussion on all papers published in Geosynthetics International. Please email your contribution to discussion@geosynthetics-international.com by 15 February 2015.